

# DRAFT SF 298

1. Report Date (dd-mm-yy)	2. Report Type	3. Dates covered (from... to )		
1995				
4. Title & subtitle Flight Control Applications of I sub 1 Optimization		5a. Contract or Grant #		
		5b. Program Element #		
6. Author(s)		5c. Project #		
		5d. Task #		
		5e. Work Unit #		
7. Performing Organization Name & Address		8. Performing Organization Report #		
9. Sponsoring/Monitoring Agency Name & Address		10. Monitor Acronym		
		11. Monitor Report #		
12. Distribution/Availability Statement Distribution approved for Public Release, Distribution Unlimited				
13. Supplementary Notes TR downloaded from a WWW unrestricted URL.				
14. Abstract				
19970121 165				
15. Subject Terms				
Security Classification of			19. Limitation of Abstract	20. # of Pages
16. Report Unclass	17. Abstract Unclass	18. This Page Unclass	Unlimited	21. Responsible Person (Name and Telephone #)

# Flight Control Applications of $\ell_1$ Optimization\*

Mark Spillman<sup>†</sup> and D. Brett Ridgely<sup>‡</sup>

Air Force Institute of Technology

Wright-Patterson AFB, Ohio

## Abstract

The  $\ell_1$  optimization method is used to handle tracking issues in the design of discrete flight controllers for a SISO aircraft longitudinal control problem. The  $\ell_1$  optimization approach is discussed theoretically and on a broad conceptual level. Constraints are developed to handle control deflection and rate limitations, overshoot and undershoot limitations and steady-state error requirements. The effect of each constraint is evaluated with simulations of the aircraft model. A closed-loop model-matching design is also presented which produces acceptable tracking results with a lower order controller.

## Introduction

A great deal of research in optimal flight control design in recent years has focused on  $H_2$  and  $H_\infty$  optimization<sup>1</sup>. While both methods work well for specific classes of inputs, neither method adequately handles “hard” magnitude and time domain constraints on the system, such as control deflection limitations, control rate limitations and overshoot restrictions in the system response. The  $\ell_1$  optimization method<sup>2</sup>, which minimizes the maximum magnitude of a system’s output to an unknown but bounded magnitude input, can be used to incorporate “hard” magnitude constraints on the system. Since this optimization method is a time domain approach, it can also address time domain constraints on the system response.

Dahleh and Diaz-Bobillo<sup>2</sup> have done the most comprehensive work on  $\ell_1$  optimization to date. In their work, they pose the  $\ell_1$  optimization problem as a linear programming

---

\*This paper is declared a work of the U.S. Government and is not subject to copyright protection in the United States. This work was sponsored in part by AFOSR.

<sup>†</sup>Currently a Stability and Control Engineer at Wright Laboratory, WL/FIGC, Bldg. 146, 2210 Eighth Street, Suite 21, WPAFB, OH 45433-7531. Email: [mspilla@falcon.flight.wpafb.af.mil](mailto:mspilla@falcon.flight.wpafb.af.mil). Member AIAA.

<sup>‡</sup>Assistant Professor, Aeronautics and Astronautics Dept., 2950 P Street, Bldg. 640, WPAFB, OH 45433-7765. Email: [dridgely@afit.af.mil](mailto:dridgely@afit.af.mil). Senior Member AIAA.

problem and solve it exactly for one block systems. Three methods for finding approximate solutions to multi-block problems are also presented. Dahleh and Diaz-Bobillo propose several methods of incorporating control deflection limitations, control rate limitations and overshoot; however, some implementation details are omitted, and few comparisons between the different methods are shown. The purpose of this paper is to investigate and compare different magnitude and time domain constraints that can be added to the  $\ell_1$  optimization problem to produce systems with good tracking characteristics. A one-block model matching design is also investigated to see if a system with good tracking qualities can be obtained with a lower order controller. MATLAB<sup>TM</sup> software written by Diaz-Bobillo<sup>3</sup> was modified and used to conduct the research in this paper.

### $\ell_1$ Optimization

The  $\ell_1$  optimization problem was first introduced by Vidyasagar<sup>4</sup>, but Dahleh and Pearson<sup>5</sup> are responsible for its more general solution. The goal of this section is to explain Dahleh and Pearson's method of solution which involves posing the problem as a linear programming problem. To simplify the explanation, the introductory development considers the case of one-block problems only. The changes necessary to find solutions to multi-block problems are discussed thereafter.

The discrete system in Figure 1, where  $r(k) \in \mathbb{R}^n$  is an exogenous input sequence of unknown but bounded magnitude and  $m(k) \in \mathbb{R}^p$  is the output sequence to be controlled, represents the standard  $\ell_1$  problem. If  $\Phi \equiv F_l(P, K)$  is the closed-loop transfer function from  $m$  to  $r$ , then the objective of  $\ell_1$  optimization can be written as

$$\inf_{K \text{ stabilizing}} \|\Phi\|_1 = \inf_{K \text{ stabilizing}} \left[ \max_{1 \leq i \leq p} \sum_{j=1}^n \sum_{k=0}^{\infty} |\phi_{ij}(k)| \right] \quad (1)$$

Several steps must be taken in order to pose this as a linear programming problem. First, the nonlinear absolute value function in the norm calculation must be removed. This is accomplished by a standard change of variables used in linear programming. Let  $\Phi = \Phi^+ - \Phi^-$ , where  $\Phi^+$  and  $\Phi^-$  are sequences of  $p \times n$  matrices with positive entries. The norm calculation

can then be replaced by

$$\max_{1 \leq i \leq p} \sum_{j=1}^n \sum_{k=0}^{\infty} \left( \phi_{ij}^+(k) + \phi_{ij}^-(k) \right) \quad (2)$$

which is equal to the norm if, for every  $(i, j, k)$ , either  $\phi^+$  or  $\phi^-$  is zero. Since  $\phi^+$  or  $\phi^-$  must be zero at the optimal solution, this substitution is valid.

Before searching for the variables  $\Phi^+$  or  $\Phi^-$  which minimize the one-norm of  $\Phi$ , constraints must be imposed to ensure that the resulting  $\Phi$  will be stable and realizable. These two problems are handled with the Youla parameterization<sup>6</sup>. Using this parameterization,  $\Phi$  can be expressed as  $\Phi = H - UQV$  where  $H$ ,  $U$  and  $V$  are known, and  $Q$  is unknown (see Maciejowski<sup>7</sup> for expressions for  $H$ ,  $U$  and  $V$ ). For one block problems  $U$  and  $V$  are inner<sup>7</sup>, and thus invertible. This means that  $Q$  can be solved for directly,  $Q = U^{-1}(H - \Phi)V^{-1}$ , which makes it easy to see that  $Q$  will be stable if and only if the transfer function  $(H - \Phi)$  cancels the unstable zeros of  $U$  and  $V$ . In other words, if the unstable zeros of  $U$  and  $V$  are denoted as  $a_i$ , then  $Q$  will be stable if and only if  $\Phi(a_i) = H(a_i)$ , for  $1 \leq i \leq N$ . Further, if  $\Phi$  is written as a function of  $\lambda$ , where  $\lambda = z^{-1}$ ,

$$\hat{\Phi}(\lambda) = \sum_{k=0}^{\infty} \Phi(k) \lambda^k \quad (3)$$

then this constraint can be expressed as (for the case of simple zeros)

$$\begin{bmatrix} 1 & a_1 & a_1^2 & \cdots \\ 1 & a_2 & a_2^2 & \cdots \\ 1 & \vdots & \vdots & \cdots \\ 1 & a_N & a_N^2 & \cdots \end{bmatrix} \begin{bmatrix} \hat{\Phi}(0) \\ \hat{\Phi}(1) \\ \hat{\Phi}(2) \\ \vdots \end{bmatrix} = \begin{bmatrix} H(a_1) \\ H(a_2) \\ \vdots \\ H(a_N) \end{bmatrix} \quad (4)$$

or  $A_{feas}\Phi = b_{feas}$  which is linear in  $\Phi$ .

With the above modifications, the  $\ell_1$  optimization problem becomes

$$\begin{aligned} \inf \quad & \sum_{k=0}^{\infty} \hat{\Phi}^+(k) + \hat{\Phi}^-(k) \\ \text{subject to} \quad & A_{feas} \left( \hat{\Phi}^+(k) - \hat{\Phi}^-(k) \right) = b_{feas} \\ & \hat{\Phi}^+(k) \geq 0, \quad \hat{\Phi}^-(k) \geq 0 \end{aligned} \quad (5)$$

which is a linear programming problem with an infinite number of variables and a finite number of constraints. The corresponding dual problem has a finite number of variables and an infinite number of constraints. However, if there are no unstable zeros of  $U$  and  $V$  on the unit circle, at some large enough  $k$ ,  $a_i^k$  will be small enough that only a finite number of these constraints will be active<sup>2</sup>. Thus, the dual problem is finite dimensional, and an exact solution can be found. Further, the existence of a solution to the dual problem guarantees the existence of the same solution to the primal problem. In fact, the  $\ell_1$  optimization problem can be solved directly in the primal space by truncating the series in (5) at a large enough value.

There are a few modifications that must be made to the above formulation for multi-block problems. First of all,  $U$  and  $V$  may not be invertible. However, if the problem is nonsingular, i.e., all the controls are penalized and no measurements are perfect, then a left-inverse of  $U$  and a right-inverse of  $V$  will exist, which is all that is required. Additionally, for multi-block problems, it is the left unstable zeros of  $U$  and the right unstable zeros of  $V$  that must cancel with zeros of  $(H - \Phi)$ .

Multi-block problems have an infinite number of variables as well as an infinite number of constraints, and thus cannot be solved exactly. To counter this problem, Dahleh and Diaz-Bobillo<sup>2</sup> proposed three ways to find approximate solutions. The first method, known as the *Finitely Many Variables (FMV)* approach, constrains the polynomial solution  $\Phi$  to a fixed length. The resulting compensator provides a sub-optimal but feasible solution to the problem. The second method, known as the *Finitely Many Equations (FME)* approach, truncates the number of dual variables, which is the same as solving the primal problem with a finite number of constraints. The solution to this problem is super-optimal and infeasible. The final and most viable method is known as the *Delay Augmentation (DA)* approximation. This method is generally considered the best method to use for multi-block problems since it carries more information about the optimal solution than the other two approaches.

The *DA* approach embeds the multi-block problem into a larger one-block problem by augmenting pure delays to  $U$  and  $V$ . The resulting one-block problem, which contains extra

degrees of freedom in  $Q$ , can then be solved exactly. While the solution to this problem is super-optimal and infeasible, it serves as an upper bound to the true optimal. To get a feasible solution, the extra degrees of freedom are simply stripped out of  $Q$ . The resulting solution is sub-optimal but provides a lower bound to the optimal solution. Thus, this method produces both a feasible solution and bounds on the optimal solution.

In later sections, the standard  $\ell_1$  linear programming problem is augmented with constraints on the maximum magnitude of the controlled output to an exogenous step input. These additional constraints are posed using the vector  $\ell_\infty$  norm,

$$\|m\|_\infty = \sup_k |m(k)| \quad (6)$$

### Understanding $\ell_1$ Optimization

In order to answer the question of how best to use  $\ell_1$  optimization, it is important to first understand what  $\ell_1$  optimization is trying to accomplish. The formal mathematical definition given in the previous section is not important here; rather, a simple conceptual idea of how the method works is sufficient. By definition,  $\ell_1$  optimization attempts to minimize the absolute sum of a system's sampled pulse response. Conceptually, this optimization method works by pushing down on the pulse response from all sides. In other words, both peak-to-peak gains and long pulse responses are penalized since both tend to increase the absolute sum.

Since the primary interest in this paper is how best to use  $\ell_1$  optimization for tracking problems, it is instructive to examine the unit pulse and step responses of a simple discrete system. Consider the continuous system,

$$H(s) = \frac{1}{s+1} = \left[ \begin{array}{c|c} -1 & 1 \\ \hline 1 & 0 \end{array} \right] \quad (7)$$

which discretized at  $1/3$  Hz using a *Zero Order Hold (ZOH)* is equivalent to

$$H(z) = \left[ \begin{array}{c|c} 0.05 & 0.95 \\ \hline 1 & 0 \end{array} \right] \quad (8)$$

The sampled unit pulse response of this system is shown in Figure 2. The one-norm of this system can be calculated by inspection. The total sum of samples 1 – 4 in Figure 2 appears

to be approximately 1. Indeed, the one-norm for this system is 1. The unit step response of the system in Equation 8 is also shown in Figure 2. Notice the distinct relationship between the unit pulse response and the unit step response. If  $r$  is the sampled unit step response and  $h$  is the sampled unit pulse response, then

$$r(k) = \sum_{j=1}^k h(j) \text{ for } k = 1, 2, \dots \quad (9)$$

This relationship implies that the faster the pulse response decays to zero, the quicker the step response reaches its steady-state value. Since  $\ell_1$  optimization penalizes long pulse responses, it logically also penalizes slow unit step responses. This fact and the general relationship between the unit pulse and unit step responses are particularly important in using  $\ell_1$  optimization for tracking problems.

### Design Problem

Throughout the rest of this paper, a Single Input Single Output (SISO) longitudinal model of the AFTI F-16 is used to illustrate various tracking design issues. This particular design example has a large frequency spread in the system dynamics (fast actuator dynamics and slow phugoid modes) which makes for a rather challenging  $\ell_1$  optimization problem. The fast dynamics in the system force a fast discretization period to be chosen, while the slow dynamics ensure the system's pulse response will decay very slowly. These two factors lead to a large number of variables required to accurately described the system's pulse response.

The tracking problem is to accurately command a  $1g$  (always from trim) normal acceleration of the aircraft. The stabilator is the only control surface considered in the model, and it is limited to  $\pm 25$  degrees deflection angle and  $\pm 60$  degrees/sec deflection rate. A linear model of the aircraft is given in the Appendix.

All simulations in this paper are done with sampled-data systems, i.e., discrete controllers with continuous system models. One  $g$  normal acceleration step inputs (from trim), applied one second after simulations are started, are used to evaluate tracking performance.

## Sensitivity Minimization

The goal of most tracking problems is to minimize the error between the commanded input and the system output. This type of problem can be posed as a sensitivity minimization problem, such as the one depicted in Figure 3. For the AFTI F-16 problem, the exogenous input,  $r$ , is an unknown commanded normal acceleration input with maximum magnitude less than or equal to one, and the controlled output,  $m$ , is the weighted error between the commanded acceleration and the actual aircraft acceleration.  $K$  is the unknown compensator, and  $G$  is the unweighted plant, described in the last section.

$W_s$  is a weighting which can be used to minimize the error to a select frequency range of command signals. Choosing an appropriate  $W_s$ , however, is often a difficult task. For this reason,  $W_s$  is set to 1 in this paper and alternative methods are explored to replace the frequency weighting.

An  $\ell_1$  optimization was performed on the system in Figure 3. Since a sensitivity problem places no penalty on control usage, a small penalty,  $\mu = 1 \times 10^{-5}$ , was added to ensure the left inverse of  $U$  exists. The optimal closed-loop system has a one-norm of 2.07 and the controller is 4<sup>th</sup> order. The system response to a 1g step in normal acceleration is shown in Figure 4. The “jags” in the response are a product of the sampled-data simulation. As the sample rate increases the “jags” become less apparent.

Notice that the step response is extremely fast. This is mainly due to the fact that there was only a small penalty placed on control usage. However, as discussed in the previous section, unconstrained  $\ell_1$  optimization tends to produce very quick step responses. Plots of control usage and rate of control usage are also shown in Figure 4. The control usage does not violate the maximum deflection limits, but it is quite large for only a 1g change in normal acceleration. Since the system is linear, it is easy to see that the maximum deflection limit would be violated for a commanded 2g change in normal acceleration. The control rate violates the maximum allowable rate limitation, even for a very small command.

The controller found above would be undesirable for two reasons: first, the system tracks with a steady-state error; second, the level of performance shown in Figure 4 is unattainable

by the AFTI F-16 due to limitations in the stabilator rate of deflection. Before discussing how to handle these problems, it is important to discuss some objectives the tracking solution should achieve. The following list represents some typical factors which may be important: i) minimum error to low frequency commands; ii) no violations of control deflection and rate limitations; iii) zero steady-state error to low frequency commands; iv) minimum overshoot and undershoot; v) the quickest response possible given the above.

Item i) indicates that sensitivity minimization is the proper objective function for  $\ell_1$  optimization, but items ii)-iv) indicate that it must be done with certain constraints. Item v) is inherently built into  $\ell_1$  optimization for most problems. Methods of incorporating items ii-iv) without using sensitivity frequency weights are explored in the sequel. In general, the same problems are encountered in a weighted sensitivity design. The next section tackles item ii). It covers three different approaches for adding control deflection and rate constraints to the error minimization problem.

### Control Deflection and Rate Limitations

The previous section was concerned with solving the one-block problem

$$\inf_{K \text{ stabilizing}} \|S\|_1 \quad (10)$$

where  $S$  is the sensitivity function. This section will first examine the general two-block problem

$$\inf_{K \text{ stabilizing}} \left\| \begin{array}{c} S \\ W_c K S \end{array} \right\|_1 \quad (11)$$

where  $W_c$  is a weighting on the control usage. The added block in (11) can be used to ensure that control deflection or rate limitations are not violated.

Since the control rate limitations were violated in the last section, only rate constraints are added in this section. It turns out that once the control rate is properly constrained for the AFTI F-16, the control deflection limitations are not a problem. The ideas presented below, however, easily extend to penalizing control deflections alone or to both control rates and deflections.

In order to change the second block of (11) to a penalty on control rate instead of control usage, an appropriate weight must be chosen for  $W_c$ . Clearly the weighting must be chosen so that it effectively takes the derivative of the control signal. This problem is best handled directly in the  $z$ -domain, with

$$W_c(z) = \frac{z-1}{Tz} \quad (12)$$

where  $T$  is the sample period. This weighting function, known as the backward Euler transformation, calculates a finite difference gradient between discrete pulses. Since the weighting is in the  $z$ -domain, the continuous system must be discretized before this weight can be augmented to the problem.

The first approach to solving the rate-constrained tracking problem is to multiply each block in the two block problem by a desired level of performance. For example, if the one-norm of the first block is desired to be less than  $\gamma$  and the maximum control deflection rate is  $U_{r_{max}}$ , then the problem becomes

$$\inf_{K \text{ stabilizing}} \left\| \frac{\frac{1}{\gamma} S}{\frac{1}{U_{r_{max}}} W_c K S} \right\|_1 \quad (13)$$

If the resulting one-norm of this system is less than 1, then both levels of performance are achieved. This follows from the previous assumption that the maximum magnitude of the exogenous input is less than or equal to one. If the goal is to find a solution which has the minimum achievable  $\gamma$  without violating the maximum control rate, this is not the best approach because (13) would have to be solved iteratively for  $\gamma$  until the resulting system one-norm is exactly one.

A better approach is to solve the following problem

$$\begin{aligned} \inf_{K \text{ stabilizing}} \quad & \|S\|_1 \\ \text{subject to} \quad & \|W_c K S\|_1 \leq U_{r_{max}} \end{aligned} \quad (14)$$

In (13), the maximum absolute row sum had to be less than one to ensure the one norm of the entire system was also less than one. In (14) the individual row sums are separated, with one being minimized while the other is constrained.

Equation (14) was solved for the AFTI F-16 with control rate limitations of 200 deg/sec, 100 deg/sec, and 60 deg/sec. A plot of the system unit step response for all three constraint levels is shown in Figure 5. The slowest response with the largest steady-state error corresponds to the actual stabilator deflection rate limitation of 60 deg/sec. The responses to the other two constraint levels are shown for comparison. This type of plot can also be used for design purposes since it is easy for the designer to see how much performance can be gained if faster control actuators are obtained. Plots of the control deflections and rates are shown in Figure 5. Notice the control rates are well below their respective  $\ell_1$  constraints for a unit step input.

The one-norm of the objective and the compensator orders are shown in Table 1 for each constraint level. The order of the  $\ell_1$  optimal compensators is directly related to the support length of the pulse response, i.e., the number of time steps it takes the pulse response to decay to zero. Since the support length of the pulse response is related to the time it takes the step response to reach steady-state, it is easy to see why the controllers found using the above approach have such high orders.

The previous two approaches imposed  $\ell_1$  constraints on the control rate. This means that the constraint limitation imposed will not be exceeded for any input into the system bounded in magnitude by one. Another less conservative option is to ensure that the constraint is not exceeded for a single class of input like the step command. Unlike the  $\ell_1$  constraints, these  $\ell_\infty$  types of constraints can only be used on a finite horizon. In other words, they can only be imposed over the support length of the solution. In many cases, however, imposing these constraints over the first few time steps is sufficient.

To understand how a constraint on the step response of the system can be imposed in  $\ell_1$  optimization, recall the relationship in (9) between the unit pulse and unit step response. The step response at any particular time step is nothing more than the sum of the pulse response at that time step plus all previous time steps. Therefore, in terms of the pulse response at each time step, these constraints can be imposed with very simple Toeplitz

matrices, with ones below the main diagonal and zeros above,

$$\begin{bmatrix} 1 & 0 & \cdots & 0 \\ 1 & \ddots & \ddots & 0 \\ \vdots & \ddots & \ddots & 0 \\ 1 & 1 & 1 & 1 \end{bmatrix} \begin{bmatrix} \hat{\Phi}(0) \\ \hat{\Phi}(1) \\ \vdots \\ \hat{\Phi}(N) \end{bmatrix} \leq \begin{bmatrix} 1 \\ 1 \\ 1 \\ 1 \end{bmatrix} U_{r_{max}} \quad (15)$$

Notice that these constraints can easily be augmented to the constraints in (4).

The new problem with the augmented step input constraints becomes

$$\begin{aligned} \inf_{K \text{ stabilizing}} \quad & \|S\|_1 \\ \text{subject to} \quad & \|W_c K S w_f\|_\infty \leq U_{r_{max}} \end{aligned} \quad (16)$$

where  $w_f$  is a unit step. A plot of the AFTI F-16 normal acceleration step response for control rate constraint levels of 200 deg/sec, 100 deg/sec and 60 deg/sec is shown in Figure 6. Again, the slowest response with the largest steady-state error corresponds to a constraint of 60 deg/sec. Notice that the step responses to this type of constraint are much quicker and have less steady-state error than the  $\ell_1$  constraints. Control deflections and control rates are also shown in Figure 6. Notice that now the rates appear to hit the constraint limits, except in the 200 deg/sec case. This is due, however, to the finite differencing used on the rates. In each case, the rate constraints are active.

The one-norm of the objective and the compensator orders are shown in Table 2 for each constraint level. With this approach, quicker settling times also lead to lower order controllers. While all the step responses in this section meet some constraint level on the control rate, none of them has zero steady-state error. This issue is addressed in the next section.

### Steady-State Error and Time-Varying Exponential Weights

Near zero steady-state error to a step input can be enforced by using a weighting on sensitivity. This typically cause problems with control rate usage and overshoot, which then need to be addressed. Thus, no weight will be added to the sensitivity and zero steady-state error to a step input will be enforced by adding an equality constraint to the  $\ell_1$  optimization

problem. Recall from (9) that the final value of the step response is simply the summation of the unit pulse response over its entire support length. Therefore, zero steady-state error to a unit step input is guaranteed if the sum of the sampled unit pulse response equals zero. This is not an absolute summation like the norm calculation; it is simply a summation of the pulse response at each time step. The added equality constraint takes the form

$$\begin{bmatrix} 1 & 1 & \cdots & 1 \end{bmatrix} \begin{bmatrix} \hat{\Phi}(0) \\ \hat{\Phi}(1) \\ \vdots \\ \hat{\Phi}(N) \end{bmatrix} = 0 \quad (17)$$

This constraint was added to the problem presented in (16), with the control rate constraint equal to 60 deg/sec. The resulting solution has an objective one-norm of 3.00 and the compensator is 44<sup>th</sup> order. The system response to a 1g normal acceleration step input is shown in Figure 7 along with the control rate. Clearly, zero steady-state error is achieved, but the limit on control rate is not met at the nearly discontinuous jump just after two seconds. Notice that the response in Figure 7 is exactly the same as its counterpart in Figure 6 up until this jump. This happened because the steady-state error equality constraint was not imposed until the very last time step in the support length. In this system, imposing the constraint any earlier results in a larger one-norm, which the optimization rejects. This problem can be overcome with time-varying exponential weights on the norm calculation. Consider multiplying each sampled pulse response by  $a^{kT}$ , where  $k$  is the sample index,  $T$  is the sample period and  $a > 1$ . Since this weight gets larger as  $k$  gets larger, it effectively penalizes late errors over early ones.

The system above was rerun with a time-varying exponential weight added to the norm calculation. With  $a = 1.1$ , the objective one-norm was 3.59 and the controller was 26<sup>th</sup> order. A plot of the system response to a step input is shown in Figure 8. Adding the exponential weights increased the one-norm as expected. The weighting also decreased the settling time and thus the controller order. The step response at this point now meets all the criteria established, except the overshoot issue. This problem is discussed in the next section.

### Overshoot and Undershoot Limitations

Problems with excessive overshoot and undershoot in the step response can be handled in exactly the same manner as excessive control deflections and rate violations. To demonstrate this concept, a very small reduction is done on the overshoot for the step response shown in Figure 8. Theoretically, the overshoot can be reduced to any desired level at the expense of a slower response. However, it was extremely difficult to find a solution for the problem presented with the current  $\ell_1$  optimization software. The multi-block problem contains so many constraints and delays that calculation attempts alone are extremely expensive in terms of computer time. Further, the linear programming routine in the software has difficulty solving very large systems of equations, possibly due to scaling problems. The system response in Figure 8 has an overshoot of about 80%. An  $\ell_\infty$  type constraint on the overshoot was added to the problem to ensure that the overshoot would be less than 70% to a step input. The resulting solution had an objective one-norm of 3.40 and the controller was 28<sup>th</sup> order. A plot of the step response with the added constraint is shown in Figure 9. Figure 10 shows a Bode plot of the controller. Note the high gain at low frequency to achieve tracking, as well as the lag-lead behavior needed to keep the control usage down and respond quickly.

This step response is still less than ideal; however, all the tools to shape and constrain the response are now available. As the  $\ell_1$  optimization software becomes more reliable and efficient, a designer should be able to use all the techniques presented up to this point to find a compensator which meets all of his or her tracking requirements. Unfortunately, this compensator may be extremely high order and therefore impractical to use. It is important to note that the designs shown up to this point are not intended to represent the best ones possible. Rather, they are shown to clearly illustrate the capabilities of  $\ell_1$  optimization. The next section on model matching demonstrates one way to use  $\ell_1$  optimization and still produce controllers at or about the order of the original discrete system. Some of the problems encountered in this final design will be handled with alternatives to the methods shown up to this point.

## Model Matching

One way to counter order inflation in  $\ell_1$  optimization is to solve a one-block problem instead. Since these problems can be solved exactly, without delay augmentation, the resulting controllers tend to be much smaller (usually about the order of the unweighted plant). An added benefit to using one-block systems is that they can be solved much faster and more reliably than multi-block systems with the current  $\ell_1$  optimization software.

In many cases, however, the constraints discussed in the previous sections can not be imposed with one-block systems. Therefore, a one block system must be chosen that incorporates as many of the design criteria required for good tracking as possible. One way to accomplish this objective is to model match the design problem to a system which has the desired tracking characteristics.

A model-matching design for the SISO AFTI F-16 problem that has been discussed throughout this paper is shown in Figure 11. A small penalty on control usage, similar to the one discussed earlier, was added to the system to make the resulting  $\ell_1$  problem nonsingular. In Figure 11,  $H$  is the ideal closed-loop model given in continuous time by  $H(s) = 4/(s + 4)$ . This closed-loop model was chosen because its step response is relatively quick, has no overshoot, and no steady-state error.

The one-norm of the solution to this design problem is 0.37 and the compensator is 5<sup>th</sup> order. A plot of the AFTI F-16 step response to a commanded 1g normal acceleration change is shown in Figure 12, along with the response of the ideal model. The step response of the solution is approximately 0.37 g's larger than the step response of the ideal model at steady-state. This is due to the fact that  $\ell_1$  optimization penalizes the maximum error and thus does not care about steady-state error in this set-up. To make the system response match the ideal model's response, the commanded normal acceleration has to be multiplied by a gain. This gain is the reciprocal of the DC gain of the discrete closed-loop transfer function,

$$T_{yr}(z) = \frac{K(z)G(z)}{1 + K(z)G(z)} \quad (18)$$

For this problem, the gain equals 0.73.

Notice that with this particular approach there is no direct way to ensure the above solution will not violate control deflection and rate limitations. In this problem, the control rate limits were violated in the first few time steps. However, the closed-loop system still performs well if the step input is first passed through a continuous prefilter equal to

$$F(s) = \frac{10}{s + 10} \quad (19)$$

and a rate limiter is added to the control signal. With the added prefilter, the system sees a smooth continuous approximation of a step input, rather than a discontinuous step input. The new input is actually a more realistic representation of a pilot command.

The system was tested with the prefilter, gain adjustments on the input, and a control rate limiter set at  $\pm 60$  deg/sec. The response is shown in Figure 13. This response has no overshoot, no steady-state error and was achieved with a 5<sup>th</sup> order controller and a small gain on the input. A Bode plot of the resulting controller is shown in Figure 14. This controller does not insert high gain at low frequency, since zero steady-state error is not enforced by the controller, but rather by the command gain. This controller also has a lag-lead structure, as in the constrained sensitivity minimization case. The *Vector Gain Margins (VGM)* and *Vector Phase Margins (VPM)*<sup>8</sup> of this system are

$$-11.4 \text{ dB} \leq VGM \leq 10.4 \text{ dB}, \quad VPM = \pm 42.9^\circ$$

These margins are very high because of a “good” match to an ideal model with a “good” loop shape.

### Conclusions

This paper presented several methods of using  $\ell_1$  optimization to solve tracking problems. Specifically, constraints that could be added to the standard  $\ell_1$  problem to handle control deflection and rate limitations, zero steady-state error requirements and overshoot limitations were discussed. While these constraints theoretically allow the control designer to tailor a system’s time response, they tend to lead to multi-block problems and thus, high

order controllers. These highly constrained multi-block problems also tend to be computationally expensive and difficult to solve with the current solution techniques. If the control designer can restrict his/her design to a one-block problem, however, controller orders at or near the order of the weighted plant are possible. This due to the fact the one-block  $\ell_1$  optimization problems can be solved exactly in this case without *Delay Augmentation*. The utility of a doing a one-block  $\ell_1$  optimization design was demonstrated in this paper with a simple model-matching problem.

### References

- <sup>1</sup> Doyle, J. C., Glover, K., Khargonekar, P. P., and Francis, B. A., "State-Space Solutions to Standard  $H_2$  and  $H_\infty$  Control Problems," *IEEE Trans. on Auto. Control*, Vol. AC-34, No. 8, 1989, pp. 831-847.
- <sup>2</sup> Dahleh, M. A. and Diaz-Bobillo, I. J., *Control of Uncertain Systems*, Prentice-Hall, Englewood Cliffs, NJ, 1995.
- <sup>3</sup> Diaz-Bobillo, I. J. MATLAB<sup>TM</sup> software for solving the  $\ell_1$  optimization problem. Modified version available from the authors, 1992.
- <sup>4</sup> Vidyasagar, M., "Optimal Rejection of Persistent Bounded Disturbances," *IEEE Trans. Auto. Control*, Vol. AC-31, No. 6, 1986, pp. 527-534.
- <sup>5</sup> Dahleh, M. A. and Pearson, J. B., " $\ell_1$  Optimal Feedback Controllers for MIMO Discrete-Time Systems," *IEEE Trans. Auto. Control*, Vol. 32, No. 4, 1987, pp. 314-327.
- <sup>6</sup> Youla, D. C., Jabr, H. A., and Bongiorno, J. J., "Modern Wiener-Hopf design of optimal controllers, Part II: The multivariable case," *IEEE Trans. Auto. Control*, Vol. AC-21, pp. 319-338.
- <sup>7</sup> Maciejowski, J. M., *Multivariable Feedback Design*, Addison-Wesley Publishing Company. Inc., 1989.

<sup>8</sup> Franklin, G. F., Powell, J. D., and Emami-Naeini, A., *Feedback Control of Dynamic Systems*, Addison-Wesley, second edition, 1991.

## Appendix

The aircraft design model used in this paper consists of an actuator servo,  $G_a$ , and the linearized longitudinal equations of motion for the aircraft,  $G_p$ , referred to as the core plant. The state-space representation of the continuous system is found by concatenating the two components.

The four states in the longitudinal model are forward speed ( $u$  in ft/sec), angle of attack ( $\alpha$  in radians), pitch angle ( $\theta$  in radians), and pitch rate ( $q$  in radians/sec). The input to  $G_p$  is the stabilator deflection ( $\delta_e$  in radians) and the output is the normal acceleration ( $n_z$  in  $g'$ s).  $G_p$  is given by

$$\begin{bmatrix} \dot{u} \\ \dot{\alpha} \\ \dot{\theta} \\ \dot{q} \end{bmatrix} = \begin{bmatrix} -1.485e-2 & 3.738e+1 & -3.220e+1 & -1.794e+1 \\ -8.000e-5 & -1.491e+0 & -1.300e-3 & 9.960e-1 \\ 0.000e+0 & 0.000e+0 & 0.000e+0 & 1.000e+0 \\ -3.600e-4 & 9.753e+0 & 2.900e-4 & -1.904e+1 \end{bmatrix} \begin{bmatrix} u \\ \alpha \\ \theta \\ q \end{bmatrix} + \begin{bmatrix} 2.140e-3 \\ -1.880e-1 \\ 0.000e+0 \\ -1.904e+1 \end{bmatrix} \delta_e$$

$$n_z = \begin{bmatrix} 1.500e-3 & 3.5264e+1 & 2.720e-2 & -3.340e-1 \end{bmatrix} \begin{bmatrix} u \\ \alpha \\ \theta \\ q \end{bmatrix} + \begin{bmatrix} -4.366e+0 \end{bmatrix} \delta_e$$

The input to  $G_a$  is the commanded stabilator deflection ( $\delta_{ec}$  in radians) and the output is the stabilator deflection.  $G_a$  is given by

$$\dot{x}_a = \begin{bmatrix} -2.000e+1 \end{bmatrix} x_a + \begin{bmatrix} 2.000e+1 \end{bmatrix} \delta_{ec}$$

$$\delta_e = \begin{bmatrix} 1.000e+0 \end{bmatrix} x_a + \begin{bmatrix} 0.000e+0 \end{bmatrix} \delta_{ec}$$

The discrete aircraft plant,  $G$ , equals  $G_a G_p$  discretized at 30Hz using a *ZOH*.

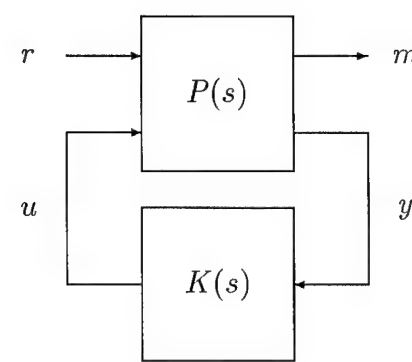


Fig. 1  $\ell_1$  optimization problem

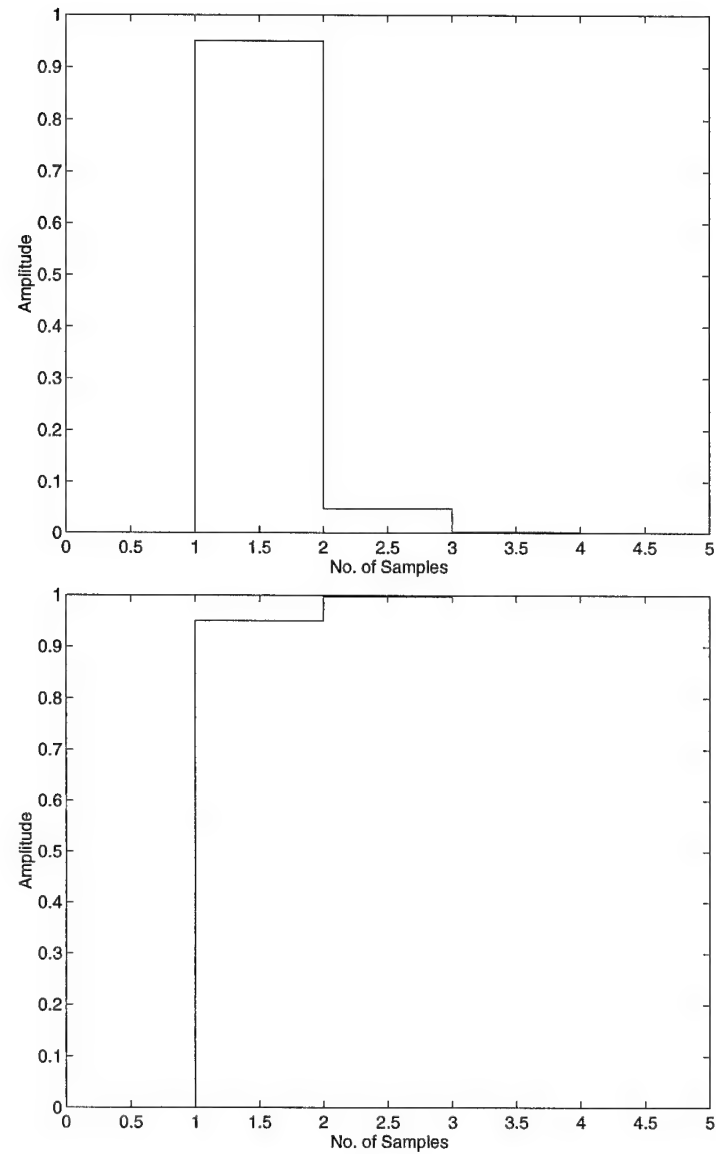


Fig. 2 Pulse (top) and step (bottom) response of a discrete system

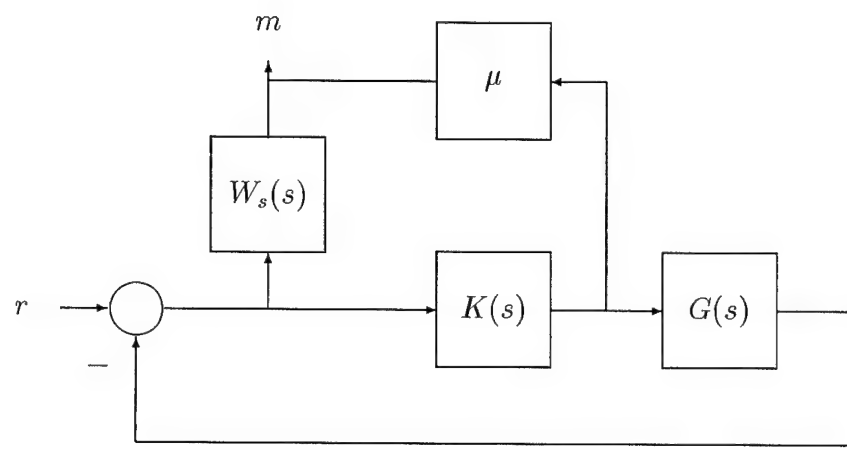


Fig. 3  $\ell_1$  sensitivity block diagram

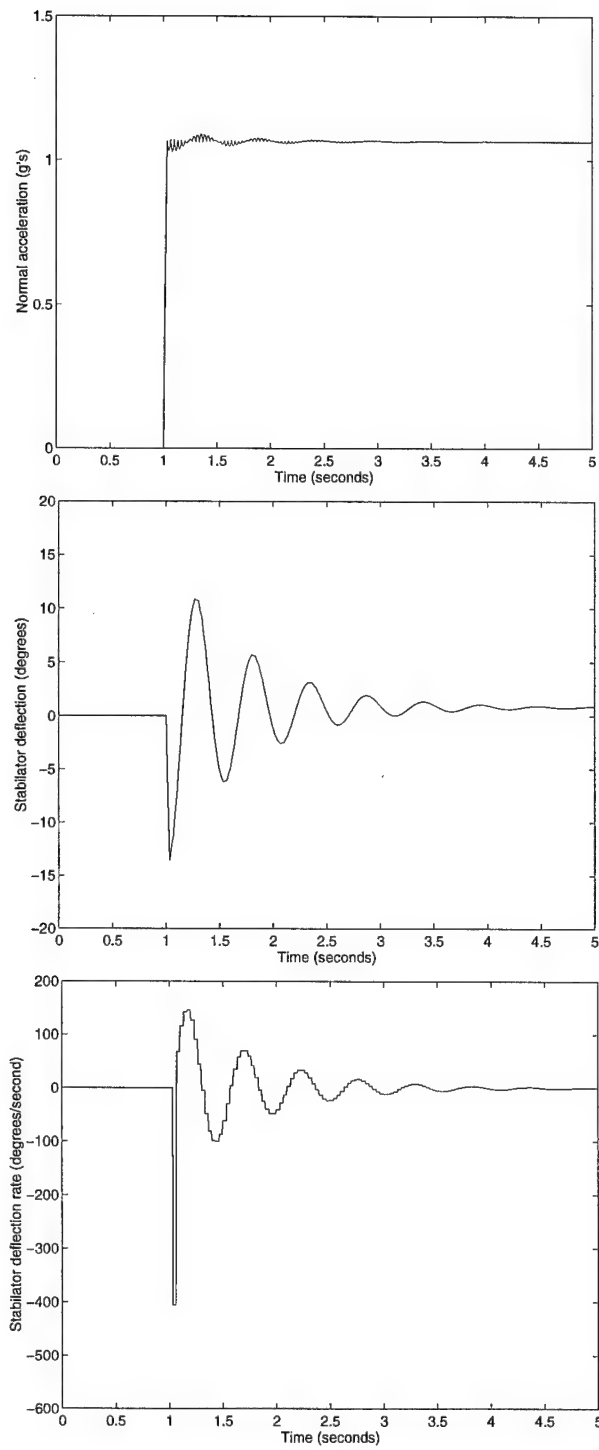
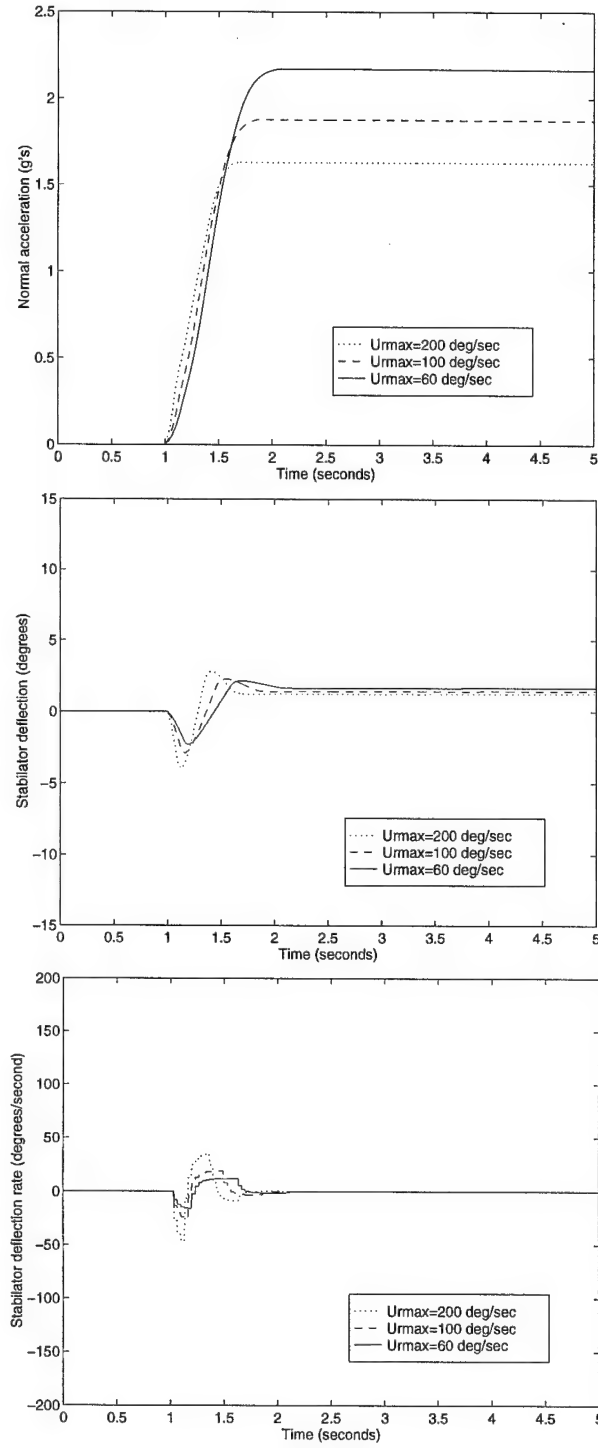
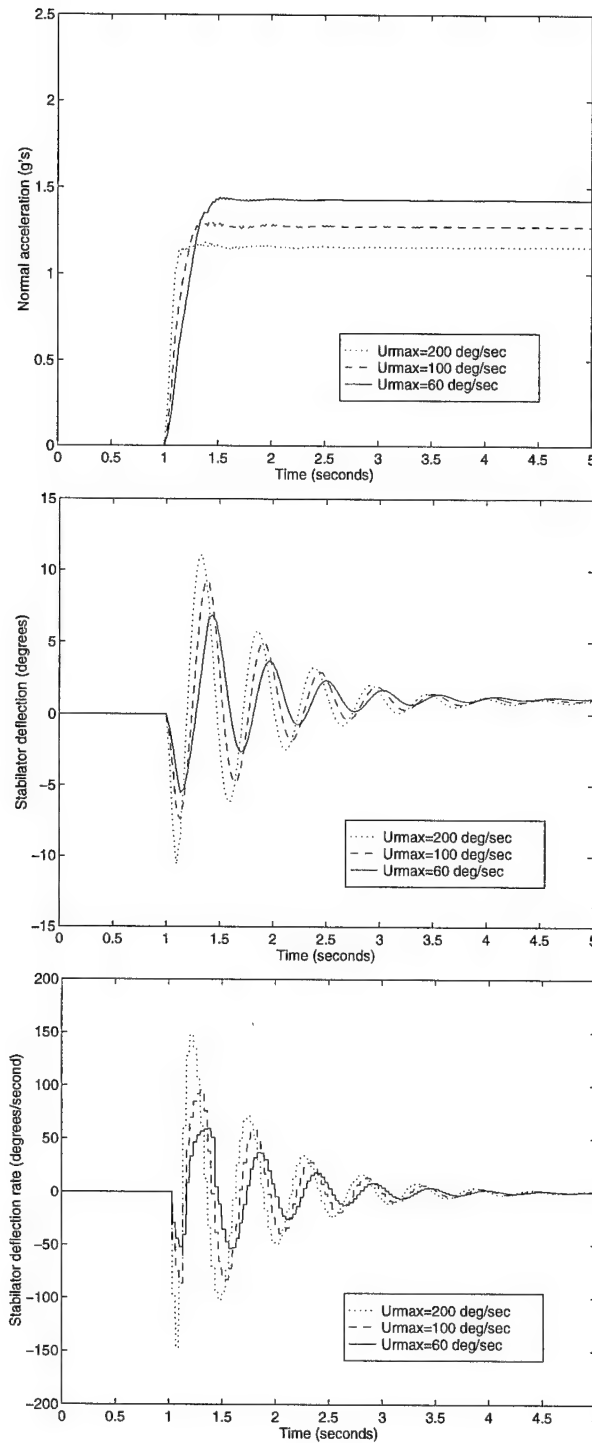


Fig. 4 Unweighted sensitivity step, control and control rate responses



**Fig. 5** Unweighted sensitivity step, control and control rate responses with  $\ell_1$  constraints on the control rate



**Fig. 6 Unweighted sensitivity step, control and control rate responses with  $\ell_\infty$  constraints on the control rate**

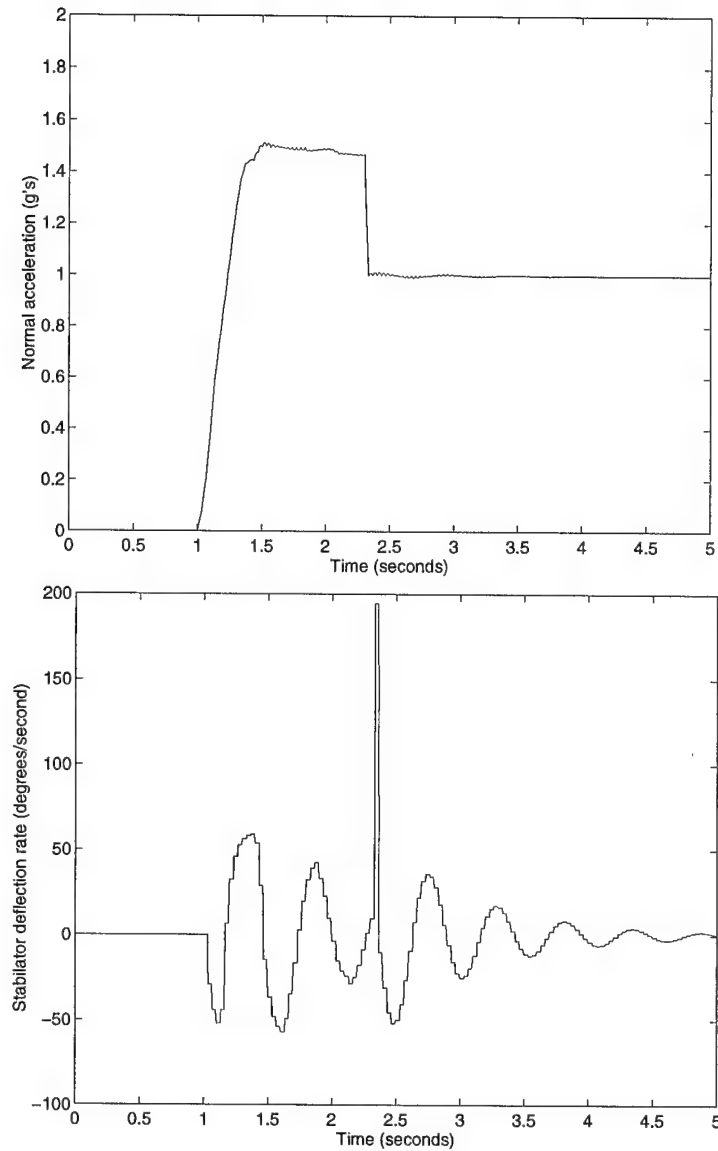


**Fig. 7** Unweighted sensitivity step and control rate responses with steady-state error and  $\ell_\infty$  control rate constraints

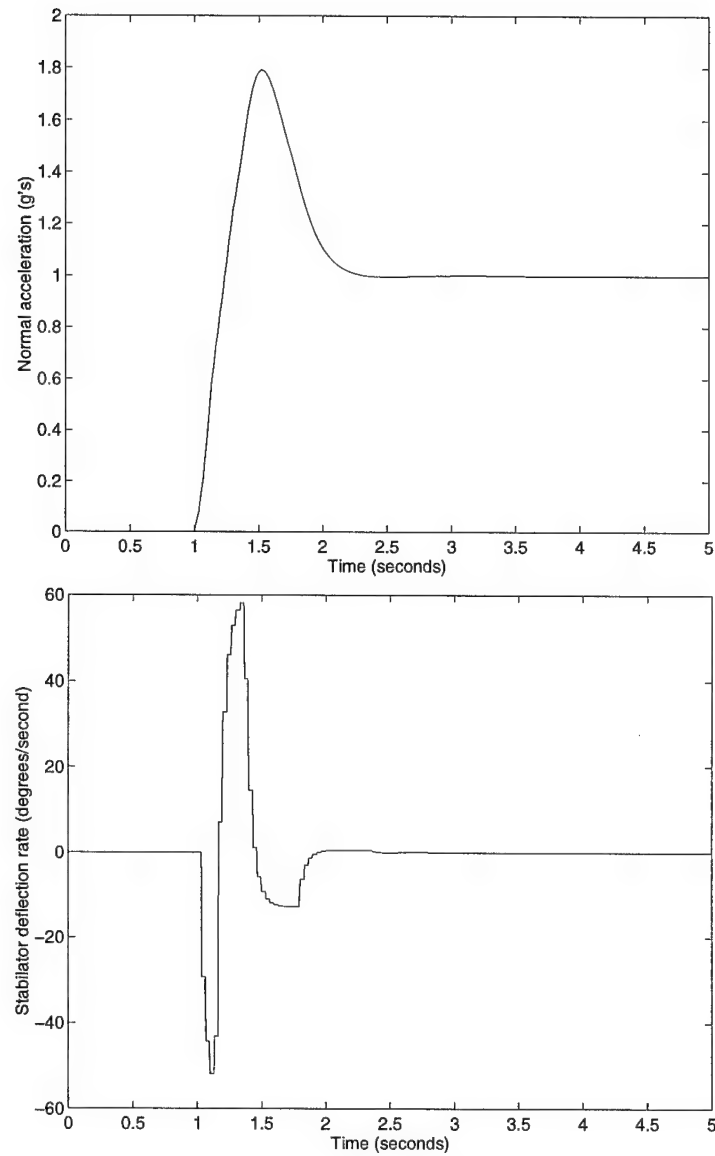
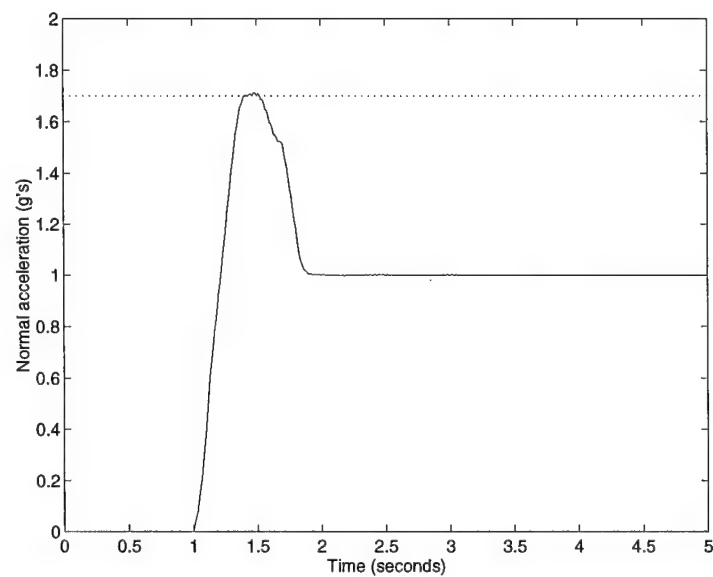
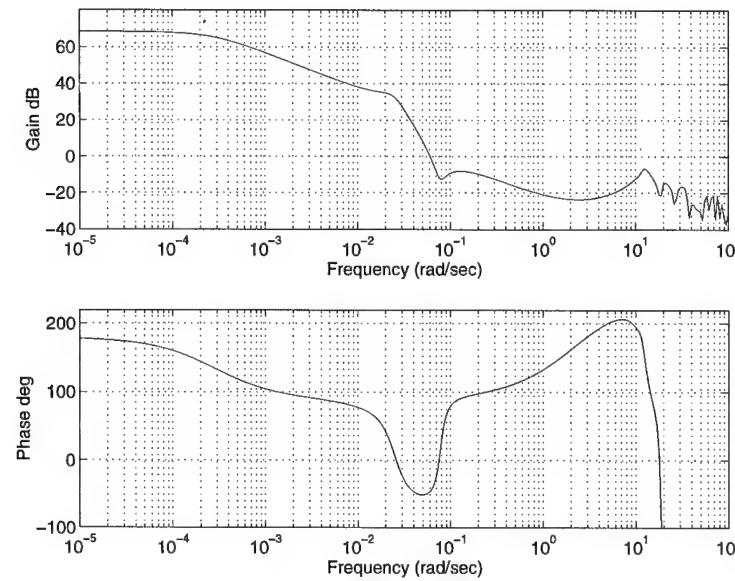


Fig. 8 Unweighted sensitivity step and control rate responses with steady-state error,  $\ell_\infty$  control rate constraints and time-varying exponential weights



**Fig. 9** Unweighted sensitivity step response with control rate, steady-state error and overshoot constraints, and time-varying exponential weights



**Fig. 10 Bode plot for the controller of Figure 9**

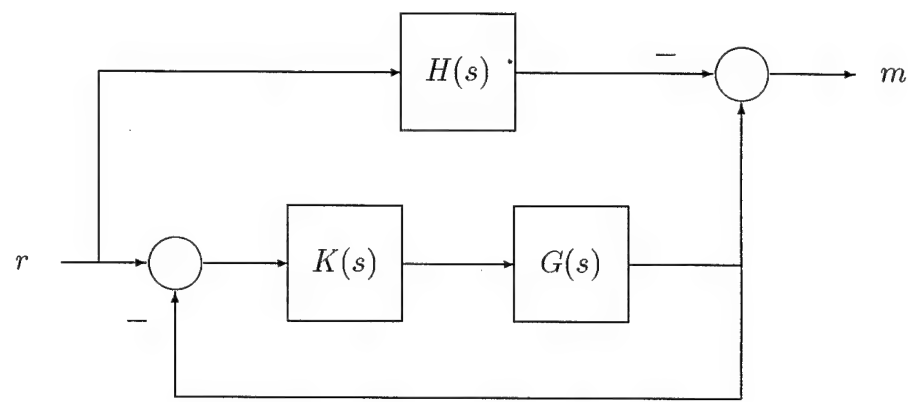
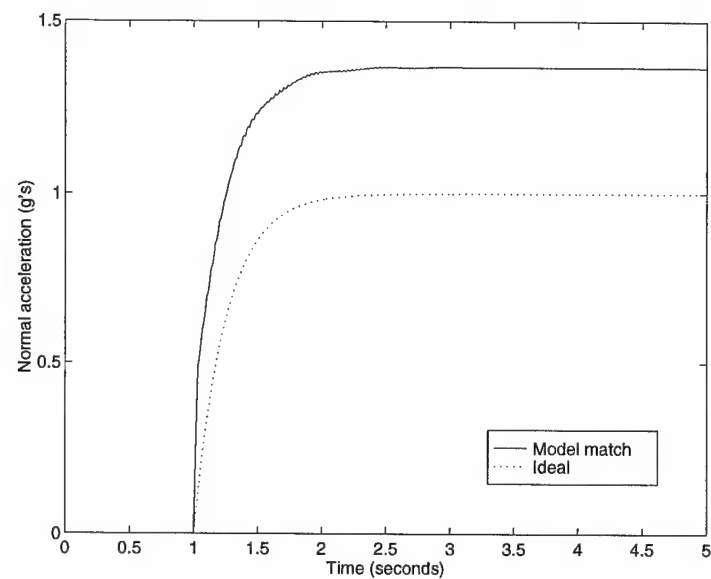
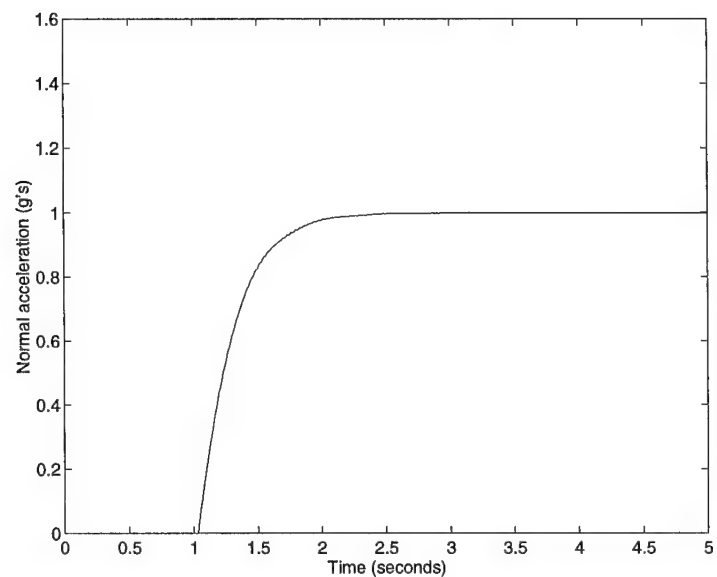


Fig. 11 Closed-loop model matching diagram



**Fig. 12 Model matching step response**



**Fig. 13** Model matching step response with scaling factor, prefilter and control rate limiter

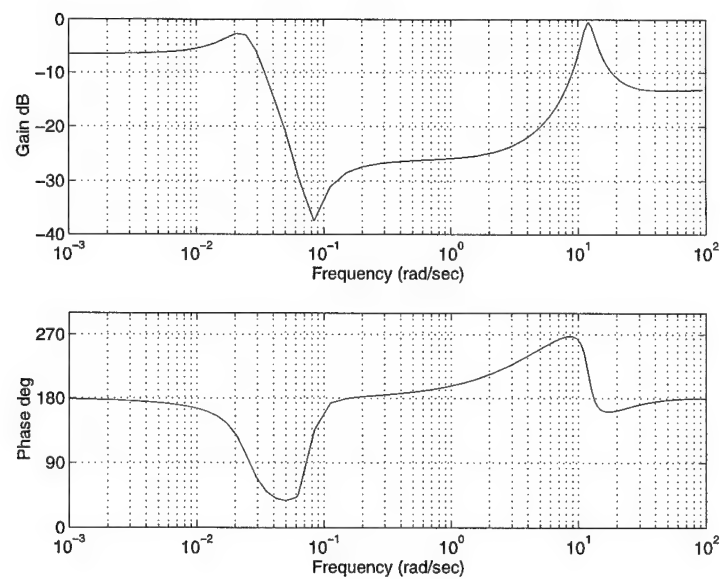


Fig. 14 Bode plot for the controller of Figure 13

**Table 1 Comparison of different  $\ell_1$  constraints on control rate**

constraint	one-norm	controller order
200 deg/sec	2.63	35
100 deg/sec	2.88	38
60 deg/sec	3.17	43

**Table 2 Comparison of different  $\ell_\infty$  constraints on control rate**

constraint	one-norm	controller order
200 deg/sec	2.16	9
100 deg/sec	2.28	13
60 deg/sec	2.43	19

## List of Figures

1	$\ell_1$ optimization problem	18
2	Pulse (top) and step (bottom) response of a discrete system	19
3	$\ell_1$ sensitivity block diagram	20
4	Unweighted sensitivity step, control and control rate responses	21
5	Unweighted sensitivity step, control and control rate responses with $\ell_1$ constraints on the control rate	22
6	Unweighted sensitivity step, control and control rate responses with $\ell_\infty$ constraints on the control rate	23
7	Unweighted sensitivity step and control rate responses with steady-state error and $\ell_\infty$ control rate constraints	24
8	Unweighted sensitivity step and control rate responses with steady-state error, $\ell_\infty$ control rate constraints and time-varying exponential weights	25
9	Unweighted sensitivity step response with control rate, steady-state error and overshoot constraints, and time-varying exponential weights	26
10	Bode plot for the controller of Figure 9	27
11	Closed-loop model matching diagram	28
12	Model matching step response	29
13	Model matching step response with scaling factor, prefilter and control rate limiter	30
14	Bode plot for the controller of Figure 13	31

### List of Tables

1	Comparison of different $\ell_1$ constraints on control rate . . . . .	32
2	Comparison of different $\ell_\infty$ constraints on control rate . . . . .	33